JCTC Journal of Chemical Theory and Computation

Article

pubs.acs.org/JCTC

Calibration of Energy-Specific TDDFT for Modeling K-edge XAS Spectra of Light Elements

Patrick J. Lestrange, Phu D. Nguyen, and Xiaosong Li*

Department of Chemistry, University of Washington, Seattle, Washington 98195, United States

Supporting Information

ABSTRACT: X-ray absorption spectroscopy (XAS) has become a powerful technique in chemical physics, because of advances in synchrotron technology that have greatly improved its temporal and spectroscopic resolution. Our recent work on energy-specific time-dependent density functional theory (ES-TDDFT) allows for the direct calculation of excitation energies in any region of the absorption spectrum, from UV-vis to X-ray. However, the ability of different density functional theories to model X-ray absorption spectra (XAS) of light elements has not yet been verified for ES-TDDFT. This work is a calibration of the ability of existing DFT kernels and basis sets to reproduce experimental K-edge excitation energies. Results were compared against 30 different transitions from gas-phase experiments. We focus on six commonly used density functionals (BHandHLYP, B3LYP, PBE1PBE, BP86, HSE06, LC-ωPBE) and various triple-ζ basis sets. The effects of core and diffuse functions are also investigated.

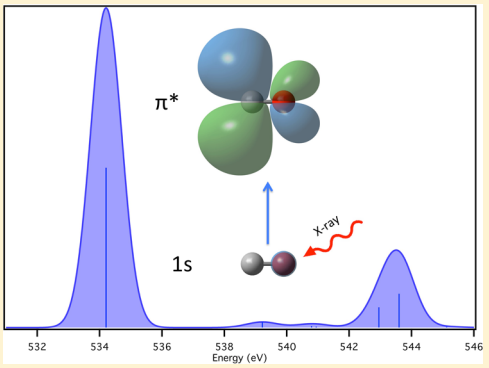

1. INTRODUCTION

Over the last few decades, X-ray absorption spectroscopy (XAS) has become a powerful tool for investigating the electronic and nuclear structure of molecules and condensed matter, because of advances in synchrotron technology that have greatly improved its temporal and spectroscopic resolution.[1−4] This technique is particularly powerful because of its ability to probe both the electronic structure (e.g., oxidation state) and the local geometry of the absorbing atom. XAS excites core electrons to weakly bound orbitals or to the continuum. The resulting spectrum contains a large absorption edge corresponding to the ionization of the core electron. The spectrum is usually partitioned into the region preceding the edge, the near-edge X-ray absorption fine structure (NEXAFS), and the region following the edge, the extended X-ray absorption fine structure (EXAFS).[5] The NEXAFS region, also known as X-ray absorption near-edge structure (XANES) for heavier elements, contains excitations to bound electronic states close to the ionization potential. The EXAFS region contains oscillatory features corresponding to the scattering of the photoelectron by the surrounding nuclei. Because XAS includes excitations to both bound and continuum states, information about both the electronic and nuclear structure of the system can be obtained in one experimental setup. As a result, X-ray spectroscopy has become increasingly prevalent in the surface science community,[6] as well as in the bioinorganic[7] and thin-film sciences.[8]

Both the NEXAFS (XANES) and EXAFS regions of the spectrum are often modeled using a scattering approach based on Green's function with muffin-tin potentials.[9,10] However, the NEXAFS region is difficult to capture without a more robust description of the electronic structure of the absorbing atom and its neighbors. The ΔSCF approach[11] and transition-potential density functional theory (DFT)[12,13] have been popular theoretical techniques for modeling NEXAFS spectra in the past. These techniques require the preparation of a full or partial core-hole in order to model core relaxation in a single determinant framework. The recent orthogonality constrained DFT method adds a proper constraint to the ΔSCF approach (where SCF stands for self-consistent field), so that single determinant core excited states are guaranteed to be orthogonal to the ground-state determinant.[14,15] In contrast, response-theory-based time-dependent density functional theory (TDDFT) does not require preparation of core−hole states and there has been much effort recently to extend this framework to model core excitations.[16−20]

There are two broadly defined implementation schemes for modeling XAS with TDDFT. One approach restricts excitations to only include the core orbitals of interest and the TDDFT equations are then solved within this reduced space. This class of method is often called restricted excitation window time-dependent density functional theory (REW-TDDFT).[16−19] The energy-specific time-dependent density functional theory (ES-TDDFT) method,[19,20] on the other hand, does not restrict the molecular orbital space when the linear response TDDFT equation is solved. Instead, the ES-TDDFT method utilizes a growing-window algorithm[21] to search for eigenvectors with eigenvalues that satisfy an energetic constraint. The ES-TDDFT method has been shown to obtain NEXAFS transition

Received: February 20, 2015

DOI: 10.1021/acs.jctc.5b00169
J. Chem. Theory Comput. XXXX, XXX, XXX−XXX

Table 1. Errors for All K-edge Transitions, Using Different Basis Set Families[a]

	K-edge Transition Data (eV)									
	Absolute Errors					Shifted Errors[b]				
	Mean AE	RMS	Max AE	MSE	Std Dev	Mean AE	RMS	Max AE	MSE	Std Dev
BP86										
6-311+G(d,p)	20.09	20.24	24.51	−20.09	2.46	1.68	1.82	2.71	−1.39	1.18
def2-TZVPD	19.93	20.09	24.54	−19.93	2.55	1.75	1.86	2.59	−1.22	1.41
aug-cc-pVTZ	20.45	20.59	24.79	−20.45	2.40	1.98	2.18	3.12	−1.97	0.94
PBE1PBE										
6-311+G(d,p)	11.36	11.43	13.79	−11.36	1.23	0.58	0.73	2.20	−0.24	0.68
def2-TZVPD	11.21	11.30	13.80	−11.21	1.41	0.72	1.05	3.62	−0.06	1.05
aug-cc-pVTZ	11.60	11.65	13.80	−11.60	1.12	0.70	0.78	1.26	−0.67	0.40
B3LYP										
6-311+G(d,p)	12.88	12.97	15.85	−12.88	1.54	0.93	1.04	2.20	−0.63	0.83
def2-TZVPD	12.72	12.83	15.84	−12.72	1.67	1.05	1.20	3.07	−0.45	1.12
aug-cc-pVTZ	13.13	13.21	15.86	−13.13	1.46	1.09	1.19	1.80	−1.06	0.55
BHandHLYP										
6-311+G(d,p)	1.92	2.06	3.87	−1.87	0.88	1.03	1.17	2.57	0.97	0.65
def2-TZVPD	1.90	2.04	3.89	−1.74	1.08	1.22	1.55	4.92	1.15	1.05
aug-cc-pVTZ	2.06	2.16	3.85	−2.06	0.65	0.73	0.82	1.62	0.65	0.51
HF										
6-311+G(d,p)	15.27	15.73	21.45	15.27	3.78	4.02	4.30	6.11	3.90	1.82
def2-TZVPD	15.29	15.75	21.28	15.29	3.78	4.10	4.50	8.66	3.97	2.11
aug-cc-pVTZ	15.08	15.52	21.25	15.08	3.67	3.78	4.09	5.93	3.65	1.84
HSE06										
6-311+G(d,p)	11.33	11.40	13.72	−11.33	1.23	0.54	0.70	2.21	−0.20	0.67
def2-TZVPD	11.18	11.27	13.73	−11.18	1.39	0.68	1.03	3.63	−0.02	1.03
aug-cc-pVTZ	11.56	11.61	13.72	−11.56	1.11	0.64	0.71	1.16	−0.60	0.38
LC-ωPBE										
6-311+G(d,p)	18.77	18.93	23.25	−18.77	2.47	0.57	0.72	2.19	−0.16	0.71
def2-TZVPD	18.57	18.76	23.17	−18.57	2.60	0.73	1.03	3.43	0.03	1.03
aug-cc-pVTZ	18.90	19.05	23.17	−18.90	2.40	0.60	0.71	1.48	−0.53	0.48

[a]Mean absolute error (Mean AE), root-mean-square (RMS) error, maximum absolute error (Max AE), mean signed error (MSE), and the standard deviation of the error are compared to experimental results.[26−32] [b]For the shifted errors, the entire spectrum is shifted, so that the lowest energy transition matches perfectly with the experiment and the errors of all other peaks are then evaluated.

energies in exact agreement with solutions obtained from the full-space TDDFT framework. The growing-window method also ensures the orthogonality of different electronic states, a condition that may fail in REW-TDDFT. Although for XAS of atomic nature, such conditions can be largely satisfied even with a restricted excitation window.[22]

In this work, we focus on calibrating the performance of the ES-TDDFT method for modeling NEXAFS with an emphasis on the dependence on density functionals and basis sets. We will examine the different levels of theory to better characterize the ability of standard density functionals to model NEXAFS. We calculate the K-edge spectra of carbon, nitrogen, and oxygen and compare our results to available experimental data. This will provide a dependable benchmark for ES-TDDFT and highlight its utility for modeling core excitations of light elements.

2. METHODOLOGY

For a detailed implementation scheme of the ES-TDDFT algorithm, we refer readers to ref 20. In this paper, we only provide a brief review of the ES-TDDFT approach. In the linear response TDDFT framework, excitation energies ω are obtained as solutions to the non-Hermitian eigenvalue equation:[21,23,24]

$$\begin{pmatrix} \mathbf{A} & \mathbf{B} \\ \mathbf{B} & \mathbf{A} \end{pmatrix}\begin{pmatrix} \mathbf{X} \\ \mathbf{Y} \end{pmatrix} = \omega\begin{pmatrix} \mathbf{1} & \mathbf{0} \\ \mathbf{0} & -\mathbf{1} \end{pmatrix}\begin{pmatrix} \mathbf{X} \\ \mathbf{Y}\boldsymbol{\delta} \end{pmatrix} \quad (1)$$

where the matrix elements of $\mathbf{A}$ and $\mathbf{B}$ are given by

$$A_{ia,jb} = \delta_{ij}\delta_{ab}(\epsilon_a - \epsilon_i) + (ia|jb) - \alpha(ib|ja) + (ia|f_{xc}|jb) \quad (2)$$

$$B_{ia,jb} = (ia|bj) - \alpha(ij|ba) + (ia|f_{xc}|bj) \quad (3)$$

Occupied and virtual molecular orbitals (MOs) are indexed by i, j and a, b respectively. The scaling factor (α) in front of the HF exchange integral has a value between 0 and 1 for hybrid functionals and 0 for pure kernels. Solving the system of linear equations as shown in eq 1 yields the first-order electron density responses $\mathbf{X}$ and $\mathbf{Y}$.

The non-Hermitian TDDFT equation in eq 1 is often recast for real orbitals into a non-Hermitian (eq 4) or a Hermitian (eq 5) problem of reduced dimension.

$$(\mathbf{A} - \mathbf{B})(\mathbf{A} + \mathbf{B})|\mathbf{X} + \mathbf{Y}\rangle = \omega^2|\mathbf{X} + \mathbf{Y}\rangle \quad (4)$$

$$(\mathbf{A} - \mathbf{B})^{1/2}(\mathbf{A} + \mathbf{B})(\mathbf{A} - \mathbf{B})^{1/2}\mathbf{T} = \omega^2\mathbf{T} \quad (5)$$

$$\mathbf{T} = (\mathbf{A} - \mathbf{B})^{-1/2}|\mathbf{X} + \mathbf{Y}\rangle \quad (6)$$

ES-TDDFT solves the Hermitian problem to obtain excitation energies using a method similar to that of Stratmann et al.[21]

DOI: 10.1021/acs.jctc.5b00169
J. Chem. Theory Comput. XXXX, XXX, XXX−XXX

Table 2. Errors for All K-edge Transitions, Focusing on the Effect of Core and Diffuse Functions[a]

	K-edge Transition Data (eV)									
	Absolute Errors					Shifted Errors[b]				
	Mean AE	RMS	Max AE	MSE	Std Dev	Mean AE	RMS	Max AE	MSE	Std Dev
BP86										
aug-cc-pVTZ	20.45	20.59	24.79	−20.45	2.40	1.98	2.18	3.12	−1.97	0.94
aug-cc-pCVTZ	20.50	20.64	24.88	−20.50	2.42	1.97	2.18	3.12	−1.97	0.93
d-aug-cc-pVTZ	20.96	21.12	25.75	−20.96	2.60	2.68	2.83	4.09	−2.68	0.93
d-aug-cc-pCVTZ	21.01	21.18	25.87	−21.01	2.63	2.69	2.85	4.08	−2.69	0.94
PBE1PBE										
aug-cc-pVTZ	11.60	11.65	13.80	−11.60	1.12	0.70	0.78	1.26	−0.67	0.40
aug-cc-pCVTZ	11.64	11.70	13.88	−11.64	1.14	0.70	0.78	1.26	−0.67	0.40
d-aug-cc-pVTZ	11.86	11.93	14.43	−11.86	1.25	1.04	1.14	1.77	−1.04	0.48
d-aug-cc-pCVTZ	11.91	11.98	14.52	−11.91	1.27	1.05	1.15	1.78	−1.05	0.48
B3LYP										
aug-cc-pVTZ	13.13	13.21	15.86	−13.13	1.46	1.09	1.19	1.80	−1.06	0.55
aug-cc-pCVTZ	13.16	13.25	15.93	−13.16	1.48	1.09	1.19	1.79	−1.06	0.55
d-aug-cc-pVTZ	13.42	13.52	16.49	−13.42	1.60	1.48	1.57	2.32	−1.48	0.54
d-aug-cc-pCVTZ	13.46	13.56	16.57	−13.46	1.62	1.49	1.58	2.32	−1.49	0.55
BHandHLYP										
aug-cc-pVTZ	2.06	2.16	3.85	−2.06	0.65	0.73	0.82	1.62	0.65	0.51
aug-cc-pCVTZ	2.09	2.19	3.87	−2.09	0.65	0.73	0.82	1.61	0.65	0.51
d-aug-cc-pVTZ	2.22	2.31	3.85	−2.22	0.62	0.57	0.68	1.50	0.42	0.53
d-aug-cc-pCVTZ	2.25	2.34	3.87	−2.25	0.62	0.57	0.68	1.51	0.42	0.54
HF										
aug-cc-pVTZ	15.08	15.52	21.25	15.08	3.67	3.78	4.09	5.93	3.65	1.84
aug-cc-pCVTZ	15.05	15.49	21.22	15.05	3.66	3.78	4.09	5.95	3.65	1.84
d-aug-cc-pVTZ	15.01	15.44	21.15	15.01	3.62	3.67	4.00	5.85	3.55	1.84
d-aug-cc-pCVTZ	14.98	15.41	21.12	14.98	3.61	3.68	4.01	5.87	3.55	1.85
HSE06										
aug-cc-pVTZ	11.56	11.61	13.72	−11.56	1.11	0.64	0.71	1.16	−0.60	0.38
aug-cc-pCVTZ	11.59	11.65	13.79	−11.59	1.13	0.64	0.71	1.15	−0.60	0.38
d-aug-cc-pVTZ	11.84	11.90	14.32	−11.84	1.24	1.00	1.09	1.64	−1.00	0.42
d-aug-cc-pCVTZ	11.88	11.95	14.41	−11.88	1.26	1.01	1.10	1.66	−1.01	0.43
LC-ωPBE										
aug-cc-pVTZ	18.90	19.05	23.17	−18.90	2.40	0.60	0.71	1.48	−0.53	0.48
aug-cc-pCVTZ	18.94	19.10	23.25	−18.94	2.43	0.60	0.71	1.48	−0.53	0.48
d-aug-cc-pVTZ	19.08	19.24	23.36	−19.08	2.46	0.78	0.93	1.66	−0.78	0.51
d-aug-cc-pCVTZ	19.11	19.28	23.43	−19.11	2.49	0.78	0.93	1.65	−0.78	0.51

[a]Mean absolute error (Mean AE), root mean square (RMS) error, maximum absolute error (Max AE), mean signed error (MSE), and the standard deviation of the error are compared to experimental results.[26−32] [b]For the shifted errors, the entire spectrum is shifted so that lowest energy transition matches perfectly with experiment and the errors of all other peaks are then evaluated.

The growing-window algorithm starts with a set of trial vectors that are associated with MO transitions above a target energy threshold, $\epsilon_a - \epsilon_i \geq \omega_0$. This energy threshold is defined based on the relevant region of the absorption spectrum. A subspace is then formed using these trial vectors, $\mathbf{C}$,

$$\tilde{\mathbf{M}}^{+} = \mathbf{C}^{\mathrm{T}}(\mathbf{A} + \mathbf{B})\mathbf{C} \tag{7}$$

$$\tilde{\mathbf{M}}^{-} = \mathbf{C}^{\mathrm{T}}(\mathbf{A} - \mathbf{B})\mathbf{C} \tag{8}$$

$$\tilde{\mathbf{M}} = (\tilde{\mathbf{M}}^{-})^{1/2}(\tilde{\mathbf{M}}^{+})(\tilde{\mathbf{M}}^{-})^{1/2} \tag{9}$$

with the dimension of $\tilde{\mathbf{M}}$ being the number of trial vectors constructed. After the diagonalization of this subspace, only the resulting eigenvalues above the energy threshold are kept. The corresponding eigenvectors are then projected back onto the full MO space so that a residual can be computed and new vectors with significant amplitude can be added into the trial vector search space. The new and expanded set of trial vectors are used to form another subspace to be diagonalized. The procedure continues until the norm of the residual is below a desired threshold and eigenvalues above the predefined energy threshold are obtained. Note that the reduced subspace is only used to generate new trial vectors and ensure solutions above the desired energy threshold. Because convergence is tested within the full MO space, the solutions of the ES-TDDFT methods are exact within the TDDFT framework.

3. RESULTS AND DISCUSSION

In this work, ES-TDDFT is used to model the K-edge absorption of light elements. Several different functional and basis set combinations were tested in order to determine an appropriate model chemistry. All calculations were carried out using a development version of Gaussian.[25] A total of 30 K-edge transitions for carbon, nitrogen, and oxygen (CO, CH_2O, C_2H_4, N_2, NH_3, NO_2) were calculated using ES-TDDFT with different functional and basis set combinations. All calculated excitation energies are compared with experimental results obtained from either gaseous X-ray absorption (XAS) or inner-

DOI: 10.1021/acs.jctc.5b00169
J. Chem. Theory Comput. XXXX, XXX, XXX−XXX

shell EELS.[26−32] Assignments are made based on the symmetry and orbital character of the transition and compared with experimental assignments. Excitation energies and assignments for all transitions can be found in the Supporting Information. In the main discussion, we only present the error analysis of excitation energies computed with different DFT kernels and basis sets.

The commonly available functionals—BHandHLYP,[33] B3LYP,[34,35] PBE1PBE,[36,37] BP86[38,39]—and two range-separated functionals (HSE06[40−42] and LC-ωPBE[43]) have been included in this study. Time-dependent HF is also included as a point of contrast.[44] All electron basis sets from three commonly used families were used: the Pople 6-311+G(d,p)[45,46] basis set, the Ahlrichs def2-TZVPD[47−50] basis set, and the Dunning aug-cc-pVTZ[51,52] basis set. In order to investigate the effect of core basis functions and diffuse functions, the singly and doubly augmented cc-pCVTZ basis sets have also been included.[53,54] All ground-state structures were optimized with the B3LYP functional and the def2-TZVP basis set. Comparisons are made using the mean absolute error (Mean AE), maximum absolute error (Maximum AE), root-mean-square (RMS) error, mean signed error (MSE), and the standard deviation of the error, with respect to experiment. Along with the absolute errors of the excitation energies, shifted errors are also reported. Because of inherent problems with DFT and the neglect of relativistic effects, DeBeer et al.[55] have proposed that relative transition energies are more chemically relevant quantities than absolute transition energies when modeling core excitations. We apply a uniform shift to the calculated spectrum such that the lowest energy peak perfectly matches the experimental value, as is done in other studies.[18,56,57] The errors are then calculated using the remaining transitions.

Table 1 shows the error analysis of predicted K-edge spectra with the ES-TDDFT method. When absolute (unshifted) errors are considered, functionals with a larger percentage of Hartree−Fock exchange result in transition energies much closer to experimental values. This is consistent with trends seen in previous studies.[18,19] BHandHLYP has 50% HF exchange (the largest percentage of HF exchange among all DFT kernels considered here) and consistently outperforms the other functionals, in terms of absolute errors with respect to experimental results. The pure density functional (BP86), with no HF exchange, significantly underestimates the K-edge excitation energies by as much as ∼26 eV, compared to only 2−4 eV error by BHandHLYP and 11−17 eV error by B3LYP, PBE1PBE, and HSE06. The performance of BHandHLYP is likely attributed to the lower self-interaction error as compared to the other functionals,[58] and error cancellations arising from the fact that TDHF consistently overestimates the excitation energies by 15−22 eV.

The two range-separated functionals tested, HSE06 and LC-ωPBE, are based off of the PBE functional and include short-range and long-range HF exchange, respectively. The HSE06 functional has comparable absolute errors to PBE1PBE (11−15 eV), but LC-ωPBE underestimates K-edge excitation energies by 18−24 eV. The inclusion of exact short-range exchange has been shown to reduce the self-interaction error and improve the description of core excitation energies while long-range exchange appears to be less important for core excitations.[58,59] Without the inclusion of short-range exchange, the transition energies calculated with LC-ωPBE are more similar to those calculated with the pure functional.

Based on the shifted errors, all hybrid functionals are much improved. The pure functional is less reliable with errors as large as ∼4 eV. Unlike absolute transition energies, the magnitude of exact exchange among hybrid functionals does not appear to be the most important factor for reproducing relative transition energies. For example, the PBE1PBE functional has the lowest shifted errors (among the functionals that are not range-separated) for several of the basis sets tested. The shifted results for TDHF are still very poor, indicating the importance of electron correlation on core excitations.

From the statistics of all K-edge excitations summarized in Tables 1 and 2, BHandHLYP clearly shows the best agreement with experimental values when absolute excitation energies are considered. When shifted results are used as in most computational practices, all hybrid functionals considered here show similarly good performance with HSE06 being the best choice, in terms of mean average errors and standard derivation.

Table 1 also shows that absolute errors of K-edge excitations are less sensitive to the quality of valence basis, compared to the shifted results. Among the three split valence basis sets considered in Table 1, aug-cc-pVTZ results have a smaller standard deviation, compared to the other two sets. As the XAS probes core electron excitations, the quality of core basis can be very important on the accuracy of computed spectrum. Flexible basis sets with a reasonable number of core functions, such as the cc-pCVTZ basis set, could improve the description of core orbital relaxation upon excitation. Diffuse functions have also been shown to have a large effect on transition energies,[60,61] so we have included the singly and doubly augmented triple-ζ Dunning basis sets with and without core functions.

Table 2 compares K-edge excitations using different basis sets with a focus on the importance of core and diffuse basis functions. The addition of more core functions seems to have little effect for these light elements as the excitation energies shift only slightly toward the experimental values. However, the average change due to these additional core functions does increase with atomic number. This suggests that core functions will be more important for heavier elements where the other functions in the set may not be capable of describing the core relaxation well. The shifted results are virtually unchanged with the addition of more core functions, differing by <0.01 eV. Diffuse functions have a slightly larger effect on the transition energies. An extra set of diffuse functions slightly increases the absolute error for all functionals, but is slightly reduced for TDHF. For the shifted spectra, the error is reduced for BHandHLYP and TDHF, but increases for all other methods with <50% HF exchange. Without a large portion of HF exchange, additional diffuse functions are not advantageous and lead to a worse description of the relative transition energies.

4. CONCLUSION

Six density functional kernels and various basis sets were used to evaluate the accuracy of ES-TDDFT for describing K-edge transitions of carbon, nitrogen, and oxygen. The results of 30 different transitions were compared against experimental values in the gas phase. There is a consistent improvement in the absolute values of the calculated excitation energies with increasing HF exchange.[18,19] Particularly, short-range exchange was shown to be an important component of any hybrid functional applied to core excitations. When shifted results are used, all hybrid functionals considered here show similarly good

DOI: 10.1021/acs.jctc.5b00169
J. Chem. Theory Comput. XXXX, XXX, XXX−XXX

performance, with HSE06 being the best choice, in terms of mean average errors and standard deviation.

For K-edge excitations of light elements, the choice of basis set does not appear to have a large effect on the absolute or shifted errors of the transition energies, and these errors are mostly dominated by the choice of the functional. Although a second set of diffuse functions seems to increase the error of the shifted spectra for all functionals with <50% HF exchange.

■ ASSOCIATED CONTENT

Supporting Information

This material is available free of charge via the Internet at http://pubs.acs.org/. The Supporting Information is available free of charge on the ACS Publications website at DOI: 10.1021/acs.jctc.5b00169.

■ AUTHOR INFORMATION

Corresponding Author

*E-mail: xsli@uw.edu.

Notes

The authors declare no competing financial interest.

■ ACKNOWLEDGMENTS

The previous development of the ES-TDDFT method was funded by the U.S. National Science Foundation (No. CHE-1265945). The application of the ES-TDDFT method to studies of X-ray absorption spectroscopy in this work is supported by the Ultrafast Initiative of the U.S. Department of Energy, Office of Science, Office of Basic Energy Sciences, through Argonne National Laboratory, under Contract No. DE-AC02-06CH11357. P.J.L. is grateful for the University of Washington Clean Energy Institute Graduate Fellowship.

■ REFERENCES

(1) Schoenlein, R.; Chattopadhyay, S.; Chong, H.; Glover, T.; Heimann, P.; Shank, C.; Zholents, A.; Zolotorev, M. *Science* **2000**, *287*, 2237−2240.
(2) Tomov, I. V.; Oulianov, D. A.; Chen, P.; Rentzepis, P. M. *J. Phys. Chem. B* **1999**, *103*, 7081−7091.
(3) Rose-Petruck, C.; Jimenez, R.; Guo, T.; Cavalleri, A.; Siders, C. W.; Rksi, F.; Squier, J. A.; Walker, B. C.; Wilson, K. R.; Barty, C. P. *Nature* **1999**, *398*, 310−312.
(4) Rischel, C.; Rousse, A.; Uschmann, I.; Albouy, P.-A.; Geindre, J.-P.; Audebert, P.; Gauthier, J.-C.; Fröster, E.; Martin, J.-L.; Antonetti, A. *Nature* **1997**, *390*, 490−492.
(5) Stöhr, J. *NEXAFS Spectroscopy*; Springer−Verlag: Berlin, Heidelberg, 2003.
(6) Nilsson, A.; Pettersson, L. G. M. *Surf. Sci. Rep.* **2004**, *55*, 49−167.
(7) Kau, L. S.; Spira-Solomon, D. J.; Penner-Hahn, J. E.; Hodgson, K. O.; Solomon, E. I. *J. Am. Chem. Soc.* **1987**, *109*, 6433−6442.
(8) Hähner, G. *Chem. Soc. Rev.* **2006**, *35*, 1244−1255.
(9) Rehr, J. J.; Albers, R. C. *Rev. Mod. Phys.* **2000**, *72*, 621−654.
(10) Rehr, J. J.; Ankudinov, A. L. *Coord. Chem. Rev.* **2005**, *249*, 131−140.
(11) Bagus, P. S. *Phys. Rev.* **1965**, *139*, A619−A634.
(12) Slater, J. C.; Johnson, K. H. *Phys. Rev. B* **1972**, *5*, 844−853.
(13) Triguero, L.; Plashkevych, O.; Pettersson, L.; Ågren, H. *J. Electron Spectrosc. Relat. Phenom.* **1999**, *104*, 195−207.
(14) Evangelista, F. A.; Shushkov, P.; Tully, J. C. *J. Phys. Chem. A* **2013**, *117*, 7378−7392.
(15) Derricotte, W. D.; Evangelista, F. A. *Phys. Chem. Chem. Phys.* **2015**, DOI: 10.1039/C4CP05509H.
(16) Stener, M.; Fronzoni, G.; de Simone, M. *Chem. Phys. Lett.* **2003**, *373*, 115−123.
(17) Ray, K.; DeBeer George, S.; Solomon, E. I.; Wieghardt, K.; Neese, F. *Chem.—Eur. J.* **2007**, *13*, 2783−2797.
(18) Besley, N. A.; Asmuruf, F. A. *Phys. Chem. Chem. Phys.* **2010**, *12*, 12024−12039.
(19) Lopata, K.; Van Kuiken, B. E.; Khalil, M.; Govind, N. *J. Chem. Theory Comput.* **2012**, *8*, 3284−3292.
(20) Liang, W.; Fischer, S. A.; Frisch, M. J.; Li, X. *J. Chem. Theory Comput.* **2011**, *7*, 3540−3547.
(21) Stratmann, R. E.; Scuseria, G. E.; Frisch, M. J. *J. Chem. Phys.* **1998**, *109*, 8218−8224.
(22) Asmuruf, F. A.; Besley, N. A. *J. Chem. Phys.* **2008**, *129*, 064705.
(23) Casida, M. E. In *Recent Advances in Density Functional Methods (Part I)*; Chong, D., Ed.; World Scientific: Singapore, 1995; pp 155−193.
(24) Dreuw, A.; Head-Gordon, M. *Chem. Rev.* **2005**, *105*, 4009−4037.
(25) Frisch, M. J.; Trucks, G. W.; Schlegel, H. B.; Scuseria, G. E.; Robb, M. A.; Cheeseman, J. R.; Scalmani, G.; Barone, V.; Mennucci, B.; Petersson, G. A.; Nakatsuji, H.; Caricato, M.; Li, X.; Hratchian, H. P.; Izmaylov, A. F.; Bloino, J.; Zheng, G.; Sonnenberg, J. L., Liang, W.; Hada, M.; Ehara, M.; Toyota, K.; Fukuda, R.; Hasegawa, J.; Ishida, M.; Nakajima, T.; Honda, Y.; Kitao, O.; Nakai, H.; Vreven, T.; J.A. Montgomery, J.; Peralta, J. E.; Ogliaro, F.; Bearpark, M.; Heyd, J. J.; Brothers, E.; Kudin, K. N.; Staroverov, V. N.; Keith, T.; Kobayashi, R.; Normand, J.; Raghavachari, K.; Rendell, A.; Burant, J. C.; Iyengar, S. S.; Tomasi, J.; Cossi, M.; Rega, N.; Millam, J. M.; Klene, M.; Knox, J. E.; Cross, J. B.; Bakken, V.; Adamo, C.; Jaramillo, J.; Gomperts, R.; Stratmann, R. E.; Yazyev, O.; Austin, A. J.; Cammi, R.; Pomelli, C.; Ochterski, J. W.; Martin, R. L.; Morokuma, K.; Zakrzewski, V. G.; Voth, G. A.; Salvador, P.; Dannenberg, J. J.; Dapprich, S.; Parandekar, P. V.; Mayhall, N. J.; Daniels, A. D.; Farkas, O.; Foresman, J. B.; Ortiz, J. V.; Cioslowski, J.; Fox, D. J. *Gaussian Development Version, Revision I.01*; Gaussian, Inc.: Wallingford, CT, 2014.
(26) Domke, M.; Xue, C.; Puschmann, A.; Mandel, T.; Hudson, E.; Shirley, D. A.; Kaindl, G. *Chem. Phys. Lett.* **1990**, *173*, 122−128.
(27) Remmers, G.; Domke, M.; Puschmann, A.; Mandel, T.; Xue, C.; Kaindl, G.; Hudson, E.; Shirley, D. *Phys. Rev. A* **1992**, *46*, 3935−3944.
(28) Tronc, M.; King, G. C.; Read, F. H. *J. Phys. B* **1979**, *12*, 137−157.
(29) Shigemasa, E.; Ueda, K.; Sato, Y.; Sasaki, T.; Yagishita, A. *Phys. Rev. A* **1994**, *45*, 2915−2921.
(30) Schirmer, J.; Trofimov, A. B.; Randall, K.; Feldhaus, J.; Bradshaw, A.; Ma, Y.; Chen, C.; Sette, F. *Phys. Rev. A* **1993**, *47*, 1136−1147.
(31) Adachi, J.-i.; Kosugi, N.; Shigemasa, E.; Yagishita, A. *J. Chem. Phys.* **1995**, *102*, 7369−7376.
(32) Püttner, R.; Dominguez, I.; Morgan, T. J.; Cisneros, C.; Fink, R. F.; Rotenberg, E.; Warwick, T.; Domke, M.; Kaindl, G.; Schlachter, A. S. *Phys. Rev. A* **1999**, *59*, 3415−3423.
(33) Becke, A. D. *J. Chem. Phys.* **1993**, *98*, 1372−1377.
(34) Becke, A. D. *J. Chem. Phys.* **1993**, *98*, 5648−5652.
(35) Stephens, P. J.; Devlin, F. J.; Chabalowski, C. F.; Frisch, M. J. *J. Phys. Chem.* **1994**, *98*, 11623−11627.
(36) Adamo, C.; Barone, V. *J. Chem. Phys.* **1999**, *110*, 6158−6170.
(37) Perdew, J. P.; Burke, K.; Ernzerhof, M. *Phys. Rev. Lett.* **1996**, *77*, 3865−3868.
(38) Becke, A. D. *J. Chem. Phys.* **1986**, *84*, 4524−4529.
(39) Perdew, J. *Phys. Rev. B* **1986**, *33*, 8822−8824.
(40) Heyd, J.; Scuseria, G. E. *J. Chem. Phys.* **2004**, *121*, 1187−1192.
(41) Heyd, J.; Scuseria, G. E. *J. Chem. Phys.* **2004**, *120*, 7274−7280.
(42) Krukau, A. V.; Vydrov, O. A.; Izmaylov, A. F.; Scuseria, G. E. *J. Chem. Phys.* **2006**, *125*, 224106.
(43) Vydrov, O. A.; Scuseria, G. E. *J. Chem. Phys.* **2006**, *125*, 234109.
(44) McWeeny, R. *Methods of Molecular Quantum Mechanics*, 2nd Edition; Academic Press: London, 1992.
(45) Krishnan, R.; Binkley, J. S.; Seeger, R.; Pople, J. A. *J. Chem. Phys.* **1980**, *72*, 650−654.
(46) Clark, T.; Chandrasekhar, J.; Spitznagel, G. W.; Schleyer, P. v. R. *J. Comput. Chem.* **1983**, *4*, 294−301.

DOI: 10.1021/acs.jctc.5b00169
J. Chem. Theory Comput. XXXX, XXX, XXX−XXX

(47) Weigend, F.; Ahlrichs, R. *Phys. Chem. Chem. Phys.* **2005**, *7*, 3297−3305.
(48) Rappoport, D.; Furche, F. *J. Chem. Phys.* **2010**, *133*, 134105.
(49) Feller, D. *J. Comput. Chem.* **1996**, *17*, 1571−1586.
(50) Schuchardt, K. L.; Didier, B. T.; Elsethagen, T.; Sun, L.; Gurumoorthi, V.; Chase, J.; Li, J.; Windus, T. L. *J. Chem. Inf. Model.* **2007**, *47*, 1045−1052.
(51) Dunning, T. H. *J. Chem. Phys.* **1989**, *90*, 1007−1023.
(52) Kendall, R. A.; Dunning, T. H.; Harrison, R. J. *J. Chem. Phys.* **1992**, *96*, 6796−6806.
(53) Woon, D. E.; Dunning, T. H. *J. Chem. Phys.* **1994**, *100*, 2975−2988.
(54) Woon, D. E.; Dunning, T. H. *J. Chem. Phys.* **1995**, *103*, 4572−4585.
(55) DeBeer George, S.; Petrenko, T.; Neese, F. *J. Phys. Chem. A* **2008**, *112*, 12936−12943.
(56) Fronzoni, G.; De Francesco, R.; Stener, M. *J. Phys. Chem. B* **2005**, *109*, 10332−10340.
(57) DeBeer George, S.; Petrenko, T.; Neese, F. *Inorg. Chem. Acta* **2008**, *361*, 965−972.
(58) Song, J.-W.; Watson, M. A.; Nakata, A.; Hirao, K. *J. Chem. Phys.* **2008**, *129*, 184113.
(59) Besley, N. A.; Peach, M. J.; Tozer, D. J. *Phys. Chem. Chem. Phys.* **2009**, *11*, 10350−10358.
(60) Wiberg, K. B.; de Oliveira, A. E.; Trucks, G. *J. Phys. Chem. A* **2002**, *106*, 4192−4199.
(61) Caricato, M.; Trucks, G. W.; Frisch, M. J.; Wiberg, K. B. *J. Chem. Theory Comput.* **2010**, *6*, 370−383.

DOI: 10.1021/acs.jctc.5b00169
J. Chem. Theory Comput. XXXX, XXX, XXX−XXX